The endocannabinoid system and pivotal role of the CB_2 receptor in mouse spermatogenesis

Paola Grimaldi[a,1,2], Pierangelo Orlando[b,c,1,2], Sara Di Siena[a], Francesca Lolicato[a], Stefania Petrosino[c,d], Tiziana Bisogno[c,d], Raffaele Geremia[a], Luciano De Petrocellis[c,e], and Vincenzo Di Marzo[c,d]

[a]Department of Public Health and Cellular Biology, University of Rome ''Tor Vergata'', 00133 Rome, Italy; [b]Institute of Protein Biochemistry (PO), Consiglio Nazionale delle Ricerche, via P. Castellino 111, Napoli, Italy; and Institutes of [d]Biomolecular Chemistry and [e]Cybernetics, and [c]Endocannabinoid Research Group, Consiglio Nazionale delle Ricerche, via Campi Flegrei 34, Pozzuoli, Italy

Edited by Ryuzo Yanagimachi, University of Hawaii, Honolulu, HI, and approved April 16, 2009 (received for review December 16, 2008)

The exact role of the endocannabinoid system (ECS) during spermatogenesis has not been clarified. We used purified germ cell fractions representative of all phases of spermatogenesis and primary cultures of spermatogonia. This approach allowed the precise quantification of the cannabinoid receptor ligands, anandamide and 2-arachidonoylglycerol, and of the expression at transcriptional and transductional levels of their metabolic enzymes and receptors. Our data indicate that male mouse germ cells possess an active and complete ECS, which is modulated during meiosis, and suggest the presence of an autocrine endocannabinoid signal during spermatogenesis. Mitotic cells possess higher levels of 2-arachidonoylglycerol, which decrease in spermatocytes and spermatids. Accordingly, spermatogonia express higher and lower levels of 2-arachidonoylglycerol biosynthetic and degrading enzymes, respectively, as compared to meiotic and postmeiotic cells. This endocannabinoid likely plays a pivotal role in promoting the meiotic progression of germ cells by activating CB_2 receptors. In fact, we found that the selective CB_2 receptor agonist, JWH133, induced the Erk 1/2 MAPK phosphorylation cascade in spermatogonia and their progression toward meiosis, because it increased the number of cells positive for SCP3, a marker of meiotic prophase, and the expression of early meiotic prophase genes.

cannabinoid receptors | meiosis | TRPV1

Since its discovery, the endocannabinoid system (ECS) has been shown to be implicated in several fundamental physiological functions as well as in many pathological conditions (1, 2). The ECS is modulated during cell proliferation, differentiation, and apoptosis through alterations of the expression levels of cannabinoid receptors (CNRs) of type 1 (CB_1) and 2 (CB_2), and of the enzymes involved in the biosynthesis and degradation of the 2 main CNR agonists: anandamide (AEA) and 2-arachidonoylglycerol (2-AG) (1). It has been demonstrated that AEA and synthetic agonists of CNRs exert antitumoral and antimetastatic activities by inhibiting cell proliferation, angiogenesis, and tumor cell migration (2).

A central role of CB_1 receptors in the regulation of the pituitary–gonad axis has been described by Wenger et al. (3), demonstrating the involvement of CB_1 in testosterone production by Leydig cells. The presence of an active ECS has been described both in testis and isolated spermatozoa of mammals, sea-urchin, and *Rana esculenta* (4–9). In particular, it has been demonstrated (6, 7) that activation of CB_1 receptors by AEA in both human and boar spermatozoa reduces their motility and the acrosomal reaction (10).

Spermatogenesis is a highly coordinated complex process characterized by mitotic (spermatogonia), meiotic (spermatocytes), and differentiative haploid (spermatids) phases. Spermatogenesis is initiated in the basal compartment of the seminiferous epithelium, by spermatogonial stem cells that proliferate and differentiate into type A1 spermatogonia. Type A1 spermatogonia undergo a series of synchronized mitotic divisions, giving rise to type B spermatogonia, which enter the meiotic phase of spermatogenesis as primary spermatocytes (11). Meiosis is characterized by two consecutive cell divisions, following a single DNA duplication, and by genetic exchange (crossing-over) between homologous chromosomes, ending up with 4 haploid round spermatids (12). Gye et al. (5), using both cryostat sections and extracts of mouse testes obtained during postnatal development, demonstrated CB_1 immunoreactivity in proliferating gonocytes and spermatozoa. Cobellis et al. (9) described the immunolocalization of CB_1 receptors in testes from the *R. esculenta* that, on the basis of seasonal considerations, the authors ascribed mainly to elongated spermatids. Another well established molecular target of AEA, the transient receptor potential vanilloid type-1 (TRPV1) channel (13), which is activated also by temperatures higher than 42 °C (14, 15), was suggested to play a role in the stabilization of the plasma membranes in capacitated sperm (7), and to confer heat resistance to male germ cells (16). Because the molecular and cellular bases of the involvement of the ECS in controlling spermatogenesis and male fertility in mammals remain unclear, the aim of this work was to investigate the presence and functional role of the ECS in germ cells at different stages of differentiation using purified germ cell fractions representative of each spermatogenesis phase (17, 18).

Results

Expression of CB_1, CB_2, and TPRV1 Receptors in Male Mouse Differentiating Germ Cells. Reverse transcription quantitative PCR (qRT-PCR) analysis (Fig. 1) showed that CB_1 receptor mRNA levels gradually increase in purified meiotic spermatocytes (SPC) and postmeiotic spermatids (SPT). CB_2 receptors showed elevated transcriptional levels in all stages of spermatogenesis with a relative peak of expression (≈10-fold increase) in SPC. The expression levels of TRPV1 showed a strong (≈100-fold) increase in meiotic cells. Protamine, a well known specific target of postmeiotic cells (19), was also evaluated as a marker of cross-contamination in isolated germ cell fractions. Protamine mRNA levels were ≈1,000 fold higher in SPC with respect to spermatogonial germ cell fraction (SPG) and showed a dramatic increase, ≈25,000-fold, in SPT (data not shown).

Because Sertoli cells (SRT) constitute the most relevant somatic contaminant (5–10%) of the mitotic germ cell fractions, we compared the transcriptional levels of CB_1, CB_2, and TRPV1 receptors in SPG fractions with those of a purified preparation of SRT. The RNA levels of all of the receptors resulted significantly lower in purified SRT (Fig. 1).

The expression of the receptors at the protein level was analyzed by Western blot analysis (WB) in cell extracts. The CB_1 receptor

Author contributions: P.G., P.O., L.D.P., and V.D.M. designed research; P.G., P.O., S.D.S., F.L., S.P., T.B., and L.D.P. performed research; P.G., P.O., R.G., L.D.P., and V.D.M. analyzed data; and P.G., P.O., R.G., L.D.P., and V.D.M. wrote the paper.

The authors declare no conflict of interest.

This article is a PNAS Direct Submission.

[1]P.G. and P.O. contributed equally to this work.

[2]To whom correspondence may be addressed. E-mail: grimaldi@uniroma2.it or p.orlando@ibp.cnr.it.

This article contains supporting information online at www.pnas.org/cgi/content/full/0812789106/DCSupplemental.

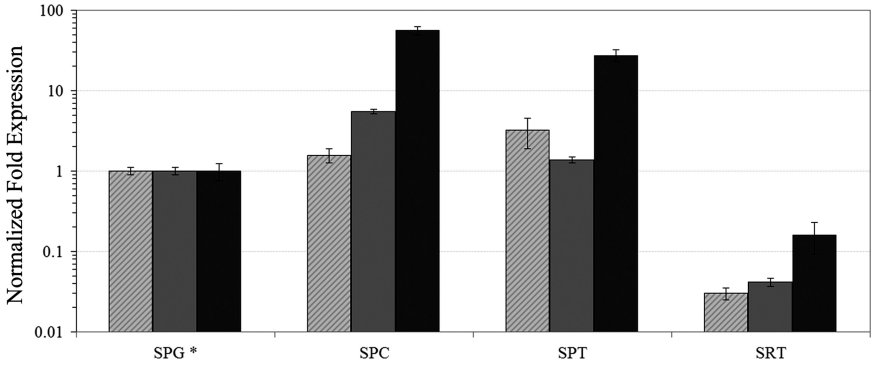

Fig. 1. CB_1,CB_2, and TRPV1 mRNA levels in mitotic, meiotic, and postmeiotic male mouse germ cells. qRT-PCR was performed as described in *Methods* using enriched fractions of premeiotic (SPG), meiotic (SPC), postmeiotic (SPT) germ cells (*A*), and Sertoli cells (SRT). The expression levels in SPG, i.e., the reference condition (*), were considered as 1 for all of the targets. The means of threshold-cycles for the reference condition were 28.9, 27.2, and 28.5 for CB1 (hatched bars), CB2 (gray bars), and TRPV1 (black bars), respectively. Standard deviations were calculated by the Gene expression module of iQ5 real-time PCR. All differences were significant ($P < 0.05$) as evaluated according to Pfaffl et al. (40). A typical experiment (R.I.N. > 8.5, see *Methods*) is depicted.

band was very faint in SPG and gradually increased in meiotic and postmeiotic germ cell extracts (Fig. S1*A*), it was detectable in cauda-epididymis spermatozoa and was absent in SRT, in agreement with previous data (4, 9). The CB_2 receptor protein was detected in all differentiative stages, and its amount was lower in SRT and undetectable in spermatozoa (SPZ) (Fig. S1*B*). The TRPV1 receptor protein was detectable in SPC and showed relatively higher levels in SPT (Fig. S1*C*). SPZ and SRT also expressed the TRPV1 receptor.

The presence of CB_2 in differentiating SPG was confirmed by immunofluorescence microscopy. Fig. 2*A* shows a strong immunostaining for this receptor, which was localized as intense punctuate fluorescence in peripheral regions of the cells and on the bridges of interconnected dividing cells as shown in Fig. 2*B*. A strong, more diffuse staining was present in SPC, whereas round SPT showed weaker staining (Fig. 2*A*). Interestingly, in elongating SPT, the immunoreactive materials accumulate in the caudal pole of the sperm where the cytoplasm is localized. At the end of spermiogenesis, when SPZ are released, the cytoplasm forms the residual bodies in which immunofluorescence was observed (Fig. 2*A*). These latter findings explain the aforementioned absence of CB_2 receptors in epididymial SPZ.

Functional CB_2 Receptors in Primary Cultures of Spermatogonia. One of the signal transduction pathways triggered by G proteins coupled to CB_1 and CB_2 receptors involves activation of the MAPK phosphorylation cascade (20, 21). The presence of a functional CB_2 receptor in SPG was evaluated by treating primary cultures of these cells with the potent selective CB_2 agonist, JWH133 (22). Treatment with different concentrations of this compound and for 15 min indicated that the optimal concentration to obtain the phosphorylation of extracellular regulated kinases (Erk1/2) MAPK was 1 μM (Fig. 3*A*). Erk1/2 activation was maintained for 30 min and then decreased to return to basal after 1 h (Fig. 3*B*). By contrast, when SPG were treated in parallel with the CB_1 specific agonist, ACEA (22) (Fig. 3*C*), Erk1/2 phosphorylation was not observed. Erk1/2 activation was also induced by the c-*kit* ligand (KL) (23). Preincubation of SPG with AM630 (10 μM), a specific CB_2 antagonist (22), antagonized the effect of JWH133 (Fig. 3*D*).

To evaluate the contribution of SRT contaminant on Erk1/2 phosphorylation induced by JWH133, we isolated pure c-*kit* expressing SPG by magnetic microbeads conjugated with CD117 and compared this preparation to a purified preparation of SRT (Fig. S2). JWH133-induced Erk1/2 phosphorylation over vehicle-treated cells was clearly lower in purified SRT, thus suggesting the little SRT contaminant could not have affected the results obtained in SPG.

JWH133 Induces Meiotic Prophase in Spermatogonia Primary Cell Cultures. To investigate whether the MAPK signal transduction pathway activated in SPG by JWH133 is related to mitotic cell cycle, we performed a morphological examination of cell nuclei from SPG treated with 1 μM JWH133 for 1 and 24 h. The number of mitotic figures (nuclei showing condensed metaphase chromosomes) did not change in presence of the agonist, suggesting that the activation of CB_2 receptors in SPG does not have a mitogenic effect (data not shown). To demonstrate whether CB_2-activated signal transduction in SPG could correlate with cell differentiation toward the meiosis prophase, we prepared nuclear spreads from these cells that were then probed with antibodies against a synaptonemal complex protein (SCP3) and a marker of meiotic nuclei (24). Fig. 4*A* shows that in control cell cultures ≈7.82 ± 1.94% of SPG naturally undergo meiotic progression after 24 h of culture. Treatment with JWH133 induced a ≈2-fold increase in the percentage of nuclei showing nuclear organization of SCP3 on meiotic chromosome figures (16.60 ± 5.54%). This effect was reversed by pretreatment of the cells with the CB_2 antagonist AM630, which did not modify the basal progression of meiosis per se. SCP3 distribution onto condensing chromatin allowed to identify different meiotic stages of prophase, as shown in Fig. 4*B*. The relative distribution of these stages in control and in agonist-treated cells are reported in Fig. 4*C*, showing that treatment of cells with JWH133 induces a ≈2-fold increase of leptotene and zygotene figures with respect to control cells, whilst inducing also the appearance of a low but consistent number of zygo-pachytene stages.

This increase in meiotic prophase was confirmed by analyzing the transcriptional levels of selected premeiotic and meiotic markers by qRT-PCR (Fig. 4*D*). The c-*Kit*, a protein expressed in SPG committed to meiotic prophase (25), increased by ≈2-fold following treatment with JWH133. Dmc1, which encodes a meiosis specific recombinase expressed during the first meiotic prophase (23), showed an increase of 1.4-fold vs. control, whereas Stra8, a protein essential for progression through the early stages of meiosis (23), increased by 1.6-fold. Lhx8, a LIM homeobox gene upregulated in KL treated spermatogonia (25), and Spo11, which is responsible for the initiation of meiotic recombination at pachytene stage through the formation of DNA double-strand breaks (23), increased not significantly.

Endocannabinoid Levels and Expression of Endocannabinoid Biosynthetic and Degradative Enzymes. SPG showed high levels of 2-AG that dramatically decreased by ≈20-fold in postmeiotic SPT, whereas AEA levels were substantially unchanged (Table 1). The transcriptional expression levels of the enzymes involved in the biosynthesis and degradation of endocannabinoids were evaluated

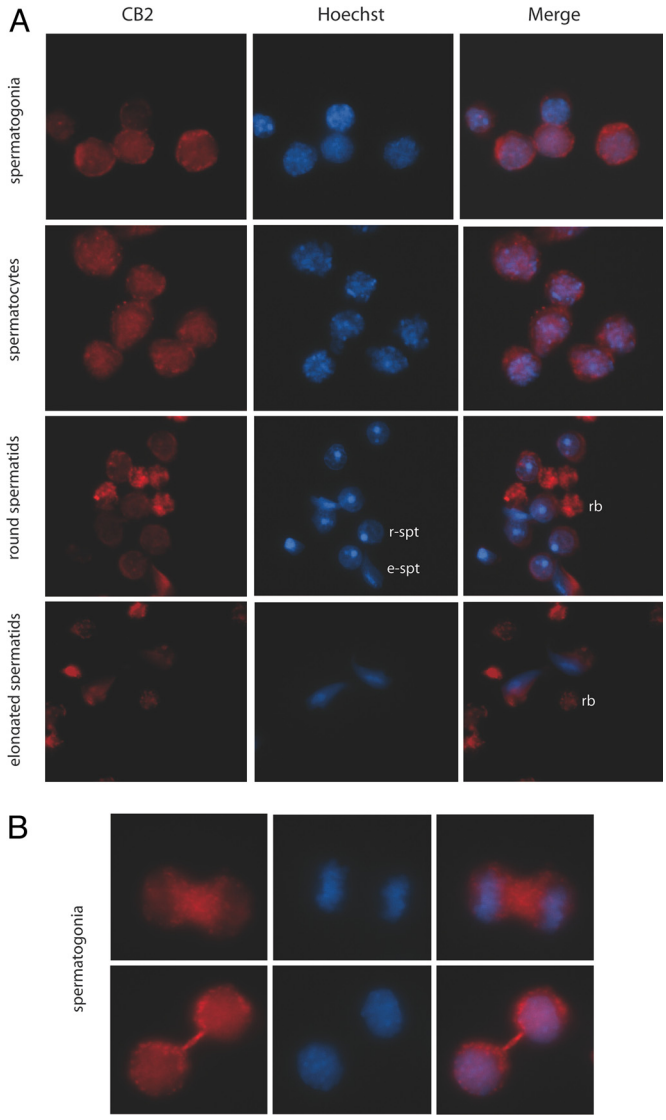

Fig. 2. CB_2 immunofluorescence staining of differentiating male germ cells. Immunofluorescence staining for CB_2 receptors (red signal), Hoechst nuclear counterstain (blue signal) and merged images of isolated testicular germ cells at different stages of differentiation. (*A*) Immunodetection of CB_2 receptors in: spermatogonia (*Top*), pachytene spermatocytes (*Middle*) and round (r-spt) and elongated (e-spt) spermatids (*Bottom*). Note that the immunofluorescence is also localized in vescicles containing only the cytoplasm that is released from the cell during spermiogenesis (residual bodies, rb); (*B*) High-magnification of CB_2 immunofluorescence pattern in dividing and interconnected spermatogonia.

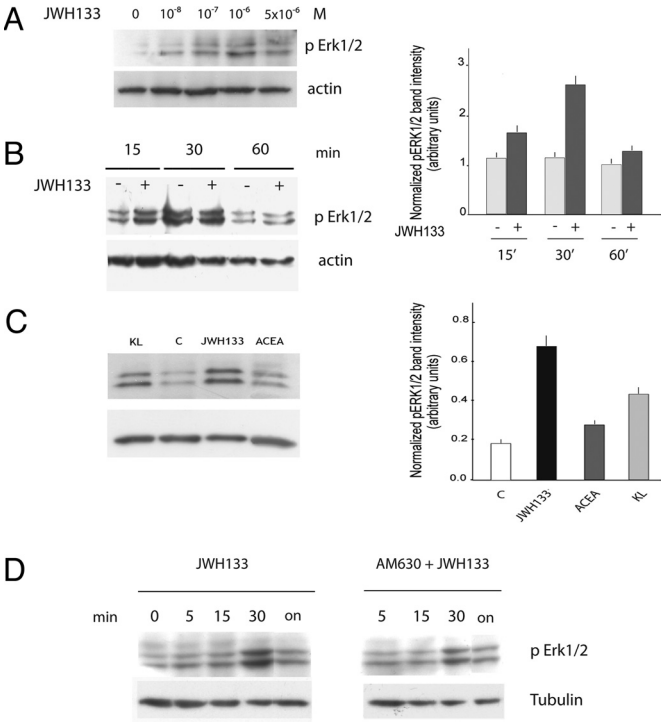

Fig. 3. MAPK signaling is activated by the CB_2 selective agonist JWH133 in spermatogonia. (*A*) Dose-dependent activation of ERK phosphorylation by JWH133 in mouse spermatogonia. Isolated mouse spermatogonia were incubated with or without 10^{-8}–5×10^{-6} M JWH133 for 15 min at 37 °C. At the end of the incubation, cell extracts were prepared and the immunoblot was performed as described in *Methods*. (*B*) Time-course analysis of JWH133-stimulated phosphorylation of ERKs in spermatogonia. Isolated spermatogonia were incubated with 10^{-6} M JWH133, for 0–60 min at 37 °C. At the end of the incubation, cell extracts were prepared for Western blot analysis with anti-phosphoERKs antibody. Densitometric analysis of phosphoERKs is shown on *Right*. (*C*) Isolated spermatogonia were treated with the CB_2-selective agonist JWH133, or with the CB_1-selecive agonist ACEA, or with c-*Kit* ligand (KL), as positive control, and pERKs activation was evaluated. Densitometric analysis is shown in *Right*. (*D*) The effects of preincubation (15 min) with the CB_2-selective antagonist AM630 (1 μM) on the phosphorylation of ERKs by JWH133 (1 μM) in mouse spermatogonia was tested at different times (5 min to 24 h).

by qRT-PCR. The mRNA levels of the two 2-AG biosynthetic diacylgycerol lipase isoenzymes (DAGL alpha and beta) (26), decreased in meiotic and postmeiotic germ cells in comparison to premeiotic germ cells (Fig. 5*A*). These data were paralleled by a relevant increase in meiotic germ cells of the 2-AG degrading enzyme, monoacylglycerol lipase (MAGL) (1) (Fig. 5*B*). The ab-hydrolase domain containing (ABDH) 6 and 12 enzymes (1), for which a role in 2-AG hydrolysis was recently proposed, were expressed in SPG at amounts comparable to MAGL levels, as judged by comparing the threshold cycles and the efficiency (see *Methods*) of the 3 PCRs (data not shown). The ABHD 12 hydrolase exhibited a modest increase of expression in meiotic and postmeiotic germ cells, whereas the levels of ABHD 6 hydrolase were unchanged.

Fig. 5*A* also shows a transcriptional increase during meiosis of *N*-acyl phosphatidylethanolamine-phosholipase D (NAPE-PLD) and fatty acid amide hydrolase (FAAH), the enzymes involved, respectively, in the biosynthesis and degradation of AEA (1). We also evaluated by enzymatic assays the DAGL, FAAH and MAGL activities during meiotic differentiation, and in SRT as a control (Table S1). Because during meiotic differentiation the size of germ cells and the content of protein and DNA varies dramatically, the most appropriate way to express specific activities is to use the cell number. The enzymatic data substantially confirmed the mRNA expression data. Comparisons of the amounts of the degrading enzymes among a mouse control tissue, SRT and the various germ cells were performed at both the protein level, by WB (Fig. S3), and by qRT-PCR (Fig. S4).

Discussion

The importance of the ECS in male reproductive functions, attested to at the phylogenetic level by its discovery in male reproductive organs of both vertebrates and invertebrates, has been pointed out in previous papers (4–8, 10, 27–30). AEA reduces sperm-fertilizing capacity in sea urchin SPZ by inhibiting the acrosome reaction (8, 28) and inhibits key fertilization fuctions such as sperm motility, capacitation, and acrosome reaction, in both boar and human (6, 7,

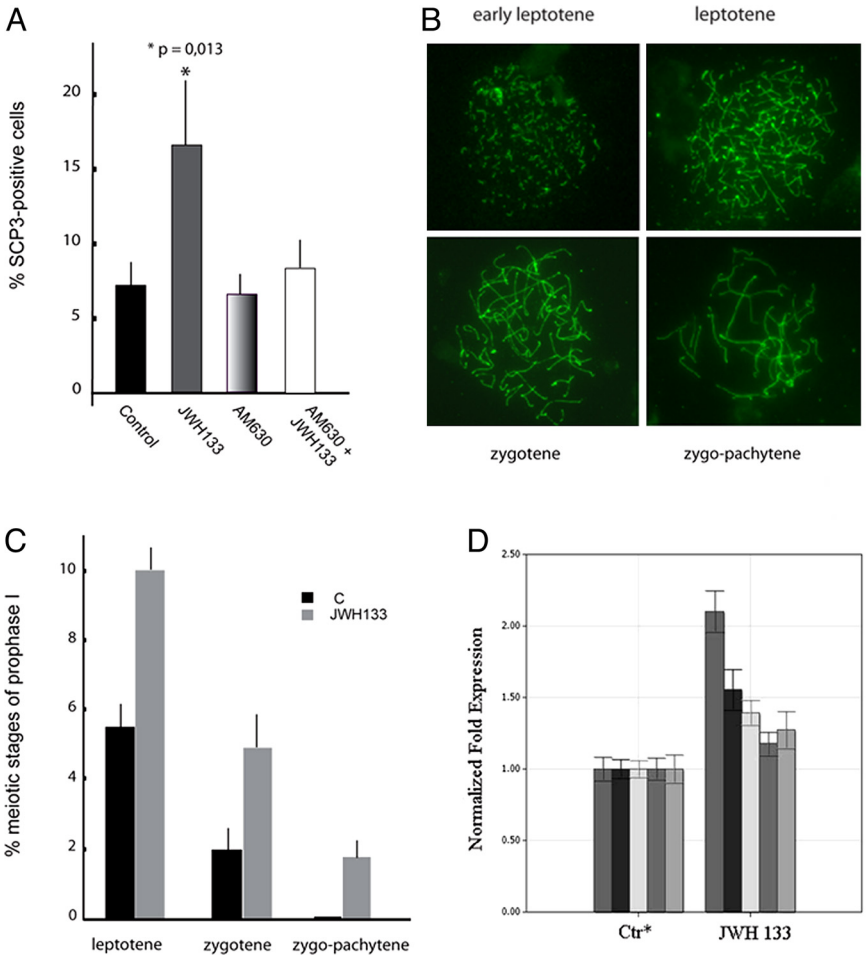

Fig. 4. JWH133 promotes differentiation of male germ cells from 7 days post partum (dpp) mice. (*A*) Histogram representing the percentage of nuclei with meiotic SCP3 staining in control testicular germ cells from 7 dpp or in cells stimulated with JWH133, AM630, or pretreated with AM630 and then treated with JWH133, after 24 h of culture. Bars represent s.d.. (*B*) Representative immunofluorescence images showing SCP3 (green) organization on nuclear spreads at the stages of early leptotene, leptotene, zygotene and zygo-pachytene of meiotic prophase, observed in 24 h cultured spermatogonia. (*C*) Percentage of leptotene, zygotene and zygo-pachytene nuclei in control cultures of germ cells from 7 dpp or in cells treated for 24 h with JWH133. Bars represent s.d. (*D*) qRT-PCR were performed as described in *Methods* in JWH133-treated premeiotic germ cells (JWH133) and untreated cells (Ctr). The expression levels in Ctr, i.e., the reference condition (*), were considered as 1 for all of the targets. The means of threshold cycles for the reference condition were 25.76, 23.21, 26.25, and 29.79 for c-*Kit* (first bar from the left), Stra-8 (second bar from the left) DMC-1 (third bar from the left), Lhx8 (fourth bar from the left), and SPO11 (last bar from the left), respectively. Standard deviations were calculated by the Gene expression module of iQ5 real-time PCR. The differences (except for Spo11 target) were significant ($P < 0.05$) as evaluated according to Pfaffl et al. (40). A typical experiment (R.I.N. $>$ 8.5, see *Methods*) is depicted.

29, 30). Ectopic synthesis of AEA and immunolocalization of the CB_1 receptor have been demonstrated in boar, human, mouse, and rat SPZ as well as in SRT and Leydig cells (4–7, 9, 29). These findings attest to the ubiquity of the ECS in the male reproductive organ and support its role in physiological functions such as the control of testosterone production and the regulation of the pituary-gonad axis (3).

Despite these several previous studies, the involvement of the ECS in spermatogenesis has been only partially explored. Cobellis et al. (9) described an increase of the expression of the CB_1 cannabinoid receptor and of FAAH in SPT of *R. esculenta.* Gye et al. (5) utilized a postpartum selection of newborn mice to obtain a selective enrichment of premeiotic, meiotic, and postmeiotic germ cells in testes. They described relatively high CB_1 expression levels in mouse testes at 1 week postpartum, which were ascribed mainly to proliferating gonocytes. CB_1 expression decreased during pre-pubertal development (2 week), increased during puberty (4 week), and reached a peak in adult testis, a picture compatible with a decrease of CB_1 mRNA transcriptional expression during meiosis, followed by an increase in postmeiotic SPT during the last transcriptional phase. Our present data confirmed an increase of CB_1 expression at both transcriptional and transductional levels in the postmeiotic fractions, although, in terms of absolute expression, low transcriptional levels were observed in premeiotic cells. However, all of the data reported so far agree with the absence of CB_1 receptors in SPG and with an increase of these receptors in mature SPT. Regarding TRPV1 channels, which are expressed in both sperm germ cells and SPZ (7, 16), we observed here a strong increase of mRNA expression in SPC and SPT, paralleled by increased TRPV1 protein levels from meiotic germ cells to differentiating round SPT. This result is important in view of the recent observation that TRPV1 plays a crucial role in the defense of testis against heat stress (16), and suggests for this receptor a protective role in meiotic progression, in addition to its regulatory function in sperm capacitation (7).

Table 1. Endocannabinoid levels in pre-meiotic, meiotic and post-meiotic male mouse germ cells

	AEA (pmoles ± SD)	2-AG (pmoles ± SD)
Spermatogonia	0.68 ± 0.13	100.65 ± 6.83
Spermatocytes	0.51 ± 0.23	44.13 ± 16.14
Spermatids	0.22 ± 0.11	5.84 ± 1.72

AEA and 2-AG were evaluated by LC-MS on enriched fractions of premeiotic (Spermatogonia), meiotic (Spermatocytes), and postmeiotic (Spermatids) male mouse germ cell fractions, as described in *Methods*. The data are the mean of 4 independent determinations in duplicate experiments. pmol values were normalized for 1×10^7 cells. s.d., standard deviation.

The present study, however, was mostly focused on the possible role of CB_2 receptors in spermatogenesis, a possibility that was recently hypothesized (31) but not yet investigated. Our findings clearly show, at both transcriptional and transductional levels, the presence of CB_2 receptors in male germ cells from mitotic SPG to haploid SPT. Interestingly, at the end of spermiogenesis, the CB_2 protein is released into the residual body and is not detectable in mature SPZ, in agreement with previous observations (6, 32). CB_2 exhibited high transcriptional levels, as evaluated on the basis of threshold cycles, in all spermatogenesis fractions analyzed, with a relative peak of activity in meiotic fractions, possibly reflecting an

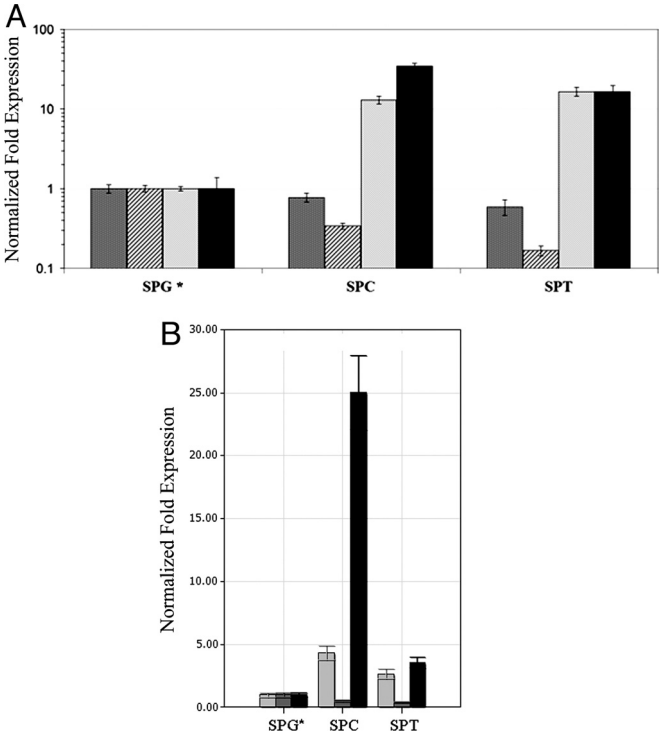

Fig. 5. Evaluation of the mRNA levels of the enzymes involved in AEA and 2-AG biosynthesis in premeiotic, meiotic and postmeiotic male mouse germ cells. qRT-PCR analyses were performed as described in *Methods* using enriched fractions of mitotic (SPG), meiotic (SPC), and postmeiotic (SPT) germ cells. The expression levels in SPG, i.e., the reference condition (*), were considered as 1 for all targets. The means of threshold cycles for the reference condition were 25.0, 25.6, 26.0, and 25.8 for DAG-alpha (light gray bar), DAG-beta (hatched bar), NAPE-PLD (stippled bar), and FAAH (black bar), respectively (*A*), and 23.09, 24.33 and 24.32 for ABHD12 (light gray bar), ABHD6 (medium gray bar), and MGLL (black bar), respectively (*B*). Standard deviations were calculated by the Gene expression module of iQ5 real-time PCR. All differences were significant ($P < 0.05$), as evaluated according to Pfaffl et al. (40). A typical experiment (R.I.N. > 8.5, see *Methods*) is depicted.

accumulation of the transcript during meiosis to be translated at later stages, a well known process occurring during spermatogenesis (33). These data seem to indicate the existence of a continuous transcriptional activity directed to assure high levels of CB_2 receptors in all phases of differentiation process.

A functional involvement of CB_2 receptors in cell differentiation was previously described in HL-60 cells transfected with CB_2 (34). CB_2 receptors and their main agonist 2-AG (AEA is less efficacious than 2-AG at these receptors) were also shown to be critical for haematopoietic cell differentiation (35). Therefore, we investigated here the effect of CB_2 activation on SPG differentiation. First of all, our data indicate the presence of a functionally active CB_2 receptor in these cells. We found that treatment of SPG with a CB_2-selective agonist activates the MAPK pathway by increasing Erk1/2 phosphorylation in a way attenuated by a CB_2-selective antagonist. Furthermore, we showed that CB_2 activation exerts a prodifferentiative effect in isolated SPG cell fractions by increasing the percentage of meiotic nuclei at all prophase stages (from leptotene to zygo-pachytene spermatocytes) and by increasing the mRNA levels of c-*kit* (23, 25), Stra8 (27, 36) and Dmc1 (23), i.e., genes that are all involved in meiotic prophase commitment and/or in meiotic progression. This study reports a prodifferentiative effect of CB_2 receptors in male germ cells.

These findings prompted us to analyze, during spermatogenesis, the levels of the main physiological CB_2 receptor ligands, AEA and 2-AG, and of the enzymes involved in their metabolism. Our data show a dramatic decrease of 2-AG levels in meiotic and postmeiotic germ cells that was paralleled by a decrease of the transcriptional and enzymatic levels of biosynthetic 2-AG enzymes, DAGL-alpha and -beta, and an increase of 2-AG degradation enzymes: MAGL, ABHD 12, and FAAH. It is noteworthy that MAGL underwent a stronger expression increase in meiotic and postmeiotic fractions with respect to ABHD 12 and FAAH, thus indicating a main role for this enzyme in 2-AG inactivation in this biological setting.

We observed a transcriptional increase during meiosis of both NAPE-PLD, one of the enzymes involved in the biosynthesis of AEA, and of the AEA-degrading FAAH. Possibly as a result, we found that the levels of AEA remained constant during spermatogenesis. It is possible that the up-regulation of AEA metabolic enzymes could serve to maintain an appropriate "anandamide tone" during meiosis as seen in mouse embryos (37). Because AEA is an agonist for TRPV1 channels, this tone would ensure the proposed TRPV1 protective action against temperature increase at the pachytene stage (16). An alternative explanation for these findings could be that NAPE-PLD mRNA is stockpiled and translated into protein in the mature SPT to ensure adequate levels of AEA that could inhibit SPZ motility during the passage through the epididymal tract (30).

In conclusion, our data demonstrate that mouse germ cells possess an active and complete ECS, which is modulated during spermatogenesis. They suggest the involvement of an autocrine endocannabinoid signal in the mitotic and meiotic phases of spermatogenesis, and indicate a pivotal role of CB_2 receptors in this process.

Methods

Male Mouse Germ Cells Isolation and Culture. Enriched SPG fractions were obtained from testes of immature 7-day-old Swiss CD-1 mice, as reported (23). Briefly, after dissection of the albuginea membrane, testes were first digested with collagenase to remove interstitial cells and then with hyaluronidase and trypsin. The cell suspension was plated in Petri dishes for 4 h in MEM supplemented with 1 mM DL-lactic acid, 2 mM sodium pyruvate, and 10% FCS to promote adhesion of somatic cells. After this preplating treatment, enriched SPG suspension was recovered, and the purity was monitored morphologically after Giemsa staining. Homogeneity of the SPG population was ≈85–90%, including all stages: undifferentiated and differentiating (type A1-A4, intermediate, and type B) SPG, 4.5% of preleptotene SPC (last S phase before meiosis), and rare leptotene SPC (23). The 10–15% contaminating cells were somatic cells (fibroblasts, myoid, and Sertoli cells).

Isolation of Kit positive SPG was performed by using magnetic-activated cell sorting (MACS) with CD117 conjugated microbeads (Miltenyi Biotec). SPG were stimulated with either JWH133 (Tocris Bioscience), or ACEA (Tocris Bioscience), or with the vehicle at different time points and then they were processed for immunofluorescence, WB or mRNA preparation. Where indicated, cells were also incubated with AM630 (Tocris Bioscience) 15 min before JWH133 addition. Testes of adult CD1 mice were used to prepare meiotic (SPC) and haploid germ cells (SPT). Germ cell suspensions were obtained by sequential collagenase-trypsin digestions of freshly withdrawn testes. Germ cells at pachytene SPC, round SPT, and elongated SPT stages were separated on the basis of their size by centrifugal elutriation in PBS containing 0.5% BSA, as described (38). The obtained SPC fraction was enriched in cells at pachytene stages (90%) and the 10% contaminating cells were round SPT, early meiotic cells, and somatic cells. The purity of the round SPT fraction was ≈90% and the 10% contaminating cells included meiotic cells, elongated SPT, and residual bodies. The elongated SPT (45–50%) were recovered in the same fraction of residual bodies (≈50%). Mature SPZ were obtained from the cauda of the epididymis of mature mice. SRT cultures were prepared as described (23).

Endocannabinoid Measurement. AEA and 2-AG were quantified by liquid chromatography–mass spectroscopy in the selected ion monitoring mode using mouse germ cell fractions containing $5–8 \times 10^{10}$ cells, as described (26). Data were means of 4 independent determinations in duplicate experiments normalized as pmols per 1×10^7 cells. Statistical analysis was performed by ANOVA followed by Bonferroni's test (StatMost).

Quantitative RT-PCR. Total RNA was extracted, analyzed by a 2100 Bionalyzer (Agilent) RNA Integrity Number (R.I.N.) >7.0 and retrotranscribed as described (39). qRT-PCR analysis was performed essentially as described by an iCycler-iQ5

CELL BIOLOGY

(Bio-Rad) in a 25-μl reaction mixture containing 10–50 ng of cDNA Optimized primers for SYBR-green analysis (GenBank accession nos.: CB_1, NM_007726; CB_2, NM_009924; TPRV1, NM_001001445; FAAH, NM_010173; NAPE-PLD, AB112350; MAGL, NM_011844; ABHD6, NM_025341; ABHD12, NM_024465; DAGL alpha, NM_198114; DAGL beta, BC016105; Stra8, NM_009292; SPO11, NM_012046; DMC1, NM_010059; c-*kit*, NM_021099; Lhx8, NM_010713) and optimum annealing temperatures were designed by Allele-Id software version 6.0 (Biosoft International) and were synthesized (HPLC-purification grade) by MWG-Biotech. Assays were performed in quadruplicate (Δ from threshold cycle of replicate samples <0.3) and a standard curve from consecutive 5-fold dilutions (100–0.16 ng) of a cDNA pool representative of all samples was included, for PCR-efficiency determination. Relative gene expression analysis, correct for PCR efficiency and normalized respect to reference genes β-actin (GenBank accession no. NM_007393) and glyceraldehyde-3-phosphate dehydrogenase (GenBank accession no. NM_008084) was performed by the iCycler-iQ5 software Gene expression module. Significance probability was evaluated according to Pfaffl et al. (40).

Western Immunoblotting and Immunofluorescence. Germ cells were lysed in 1% Triton X-100, 150 mM NaCl, 15 mM $MgCl_2$, 15 mM EGTA, 10% glycerol, 50 mM Hepes (pH 7.4) with protease inhibitors. Proteins were separated by 10% SDS/PAGE and transferred to nitrocellulose membrane (Amersham). The membrane was blocked in PBS–5% skim milk powder for 1 h. Incubation of the membrane with the primary antibody was carried out at 4 °C overnight in PBS–5% BSA and then with the appropriate HRP-conjugated secondary antibody (SantaCruz). First antibody incubation was carried out with 1:1,000 dilution of anti-CB_1 rabbit polyclonal antibody (Abcam, ab3559), 1:1,000 dilution of anti-CB_2 rabbit polyclonal antibody (Abcam, ab3561), 1:1,000 anti-TRPV1 rabbit polyclonal antibody (Abcam, ab6166), 1:1,000 anti-phospho Erk1/2 rabbit polyclonal antibody (Cell Signaling Technology, 9101), 1:500 anti-FAAH rabbit polyclonal antibody (Cayman, 101600), 1:500 anti MAGL rabbit polyclonal antibody (Cayman, 100035), anti-actin rabbit polyclonal (New England Biolabs, sc-7210). The HRP conjugate was detected by a chemioluminescence ECL kit (Amersham) and autofluorography. For immunofluorescence, germ cells were let to adhere onto polyL-lysine coated slides and permeabilized for 10 min in 0.1% Triton X-100 in PBS. After 1 h in blocking solution (5% BSA in PBS), antibodies were added at 1:100 dilution in 0.5% BSA in PBS and incubated overnight at 4 °C. Anti-rabbit Cyanin-3 secondary antibodies were added to the cells for an additional 1 h. Nuclei were labeled with Hoechst 33349 (1 μg/ml). For meiotic cell spreads, SPG were prepared and stained essentially as described (25). Slides were washed twice in PBS and incubated with anti-SCP3 rabbit polyclonal antibody (Novus NB 730F) in blocking solution (10% serum from goat, 3% BSA, 0.05% Triton X-100 in PBS), overnight at 4 °C. After washing, anti-rabbit FITC secondary antibody (Novus NB300–231) was added for 1 h at 37 °C. The slides were washed and allowed to dry. Vectashield Mounting Medium with DAPI (Vector Laboratories) was added and the slides were viewed.

Enzymatic Assays. Cells were resuspended in Tris–HCl buffer, pH 7.4 and homogenized in a Dounce homogenizer. The homogenates were centrifuged at 800 $\times$ *g* (5 min) and then at 10,000 $\times$ *g* (25 min), at 4 °C. The supernatant (cytoplasm fraction) was used for the MAGL activity assay, whereas the pellet (membrane fraction) was resuspended in the same buffer and used for DAGL and FAAH activity assays. Assays were carried out as described (26).

ACKNOWLEDGMENTS. We thank M. Pellegrini for assistance with nuclear spread preparation; P Rossi and A. Ligresti for helpful suggestions on the manuscript; and S. Piantedosi for artwork. This work was supported by the Italian Ministry of University (Grant Prin 2007 200788TPYE_002) and Ricerca Scientifica d'Ateneo (Grant RSA 2007).

1. Di Marzo V (2008) Targeting the endocannabinoid system: To enhance or reduce? *Nat Rev Drug Discov* 7:438–455.
2. Pacher P, Bátkai S, Kunos G (2006) The endocannabinoid system as an emerging target of pharmacotherapy. *Pharmacol Rev* 58:389–462.
3. Wenger T, Ledent C, Csernus V, Gerendai I (2001) The central cannabinoid receptor inactivation suppresses endocrine reproductive functions. *Biochem Biophy Res Commun* 284:363–368.
4. Maccarrone M, et al. (2003) Anandamide activity and degradation are regulated by early postnatal aging and follicle-stimulating hormone in mouse Sertoli cells. *Endocrinology* 144:20–28.
5. Gye MC, Kang HH, Kang HJ (2005) Expression of cannabinoid receptor 1 in mouse testes. *Arch Androl* 51:247–255.
6. Rossato M, Ion Popa F, Ferigo M, Clari G, Foresta C (2005) Human sperm express cannabinoid receptor Cb1, the activation of which inhibits motility, acrosome reaction, and mitochondrial function. *J Clin Endocrinol Metab* 90:984–991.
7. Maccarrone M, et al. (2005) Characterization of the endocannabinoid system in boar spermatozoa and implications for sperm capacitation and acrosome reaction. *J Cell Sci* 118:4393–4404.
8. Schuel H, Burkman LJ (2005) A tale of two cells: Endocannabinoid-signaling regulates functions of neurons and sperm. *Biol Reprod* 73:1078–1086.
9. Cobellis G, et al. (2006) Endocannabinoid system in frog and rodent testis: Type-1 cannabinoid receptor and fatty acid amide hydrolase activity in male germ cells. *Biol Reprod* 75:82–89.
10. Battista N, et al. (2008) Regulation of male fertility by the endocannabinoid system. *Mol Cell Endocrinol* 286:S17–S23.
11. de Rooij DG (2001) Proliferation and differentiation of spermatogonial stem cells. *Reproduction* 121:347–354.
12. Roeder GS (1997) Meiotic chromosomes: It takes two to tango. *Genes Dev* 11:2600–2621.
13. Zygmunt PM, et al. (1999) Vanilloid receptors on sensory nerves mediate the vasodilator action of anandamide. *Nature* 400:452–457.
14. Caterina MJ, et al. (1997) The capsaicin receptor: A heat-activated ion channel in the pain pathway. *Nature* 389:816–824.
15. Gavva NR (2008) Body-temperature maintenance as the predominant function of the vanilloid receptor TRPV1. *Trends Pharmacol Sci* 29:550–557.
16. Mizrak SC, van Dissel-Emiliani FM (2008) Transient receptor potential vanilloid receptor-1 confers heat resistance to male germ cells. *Fertil Steril* 90:1290–1293.
17. Orlando P, Geremia R, Frusciante C, Tedeschi B, Grippo P (1988) DNA repair synthesis in mouse spermatogenesis involves DNA polymerase beta activity. *Cell Differ* 23:221–230.
18. Pellegrini M, Grimaldi P, Rossi P, Geremia R, Dolci S (2003) Developmental expression of BMP4/ALK3/SMAD5 signaling pathway in the mouse testis: A potential role of BMP4 in spermatogonia differentiation. *J Cell Sci* 116:3363–3372.
19. Ravel C, et al. (2007) Mutations in the protamine 1 gene associated with male infertility. *Mol Hum Reprod* 13:461–464.
20. Bouaboula M, et al. (1996) Signaling pathway associated with stimulation of CB2 peripheral cannabinoid receptor. Involvement of both mitogen-activated protein kinase and induction of Krox-24 expression. *Eur J Biochem* 237:704–711.
21. Melck D, et al. (1999) Involvement of the cAMP/protein kinase A pathway and of mitogen-activated protein kinase in the anti-proliferative effects of anandamide in human breast cancer cells. *FEBS Lett* 463:235–240.
22. Fowler CJ (2008) ''The tools of the trade''–an overview of the pharmacology of the endocannabinoid system. *Curr Pharm Des* 14:2254–2265.
23. Pellegrini M, et al. (2008) ATRA and KL promote differentiation toward the meiotic program of male germ cells. *Cell Cycle* 7:3878–3888.
24. Saunders PT, et al. (2003) Absence of mDazl produces a final block on germ cell development at meiosis. *Reproduction* 126:589–597.
25. Rossi P, et al. (2008) Transcriptome analysis of differentiating spermatogonia stimulated with kit ligand. *Gene Expr Patterns* 8:58–70.
26. Bisogno T, et al. (2003) Cloning of the first sn1-DAG lipases points to the spatial and temporal regulation of endocannabinoid signaling in the brain. *J Cell Biol* 163:463–468.
27. Dalterio S, Badr F, Bartke A, Mayfield D (1982) Cannabinoids in male mice: Effects on fertility and spermatogenesis. *Science* 216:315–316.
28. Schuel H, Goldstein E, Mechoulam R, Zimmerman AM, Zimmerman S (1994) Anandamide (arachidonylethanolamide), a brain cannabinoid receptor agonist, reduces sperm fertilizing capacity in sea urchins by inhibiting the acrosome reaction. *Proc Natl Acad Sci USA* 91:7678–7682.
29. Schuel H, et al. (2002) Evidence that anandamide-signaling regulates human sperm functions required for fertilization. *Mol Reprod Dev* 63:376–387.
30. Ricci G, et al. (2007) Endocannabinoid control of sperm motility: The role of epididymus. *Gen Comp Endocrinol* 153:320–322.
31. Maccarrone M (2008) CB2 receptors in reproduction. *Br J Pharmacol* 153:189–198.
32. Sun X, et al. (2009) Genetic loss of Faah compromises male fertility in mice. *Biol Reprod* 80:235–242.
33. Monesi V (1965) Synthetic activities during spermatogenesis in the mouse RNA and protein. *Exp Cell Res* 9:197–224.
34. Derocq JM, et al. (2000) Genomic and functional changes induced by the activation of the peripheral cannabinoid receptor CB2 in the promyelocytic cells HL-60. Possible involvement of the CB2 receptor in cell differentiation. *J Biol Chem* 275:15621–15628.
35. Catani MV, et al. (2009) Expression of the endocannabinoid system in the bi-potential HEL cell line: Commitment to the megakaryoblastic lineage by 2 arachidonoylglycerol. *J Mol Med* 87:65–74.
36. Baltus AE, et al. (2006) In germ cells of mouse embryonic ovaries, the decision to enter meiosis precedes premeiotic DNA replication. *Nat Genet* 38:1430–1434.
37. Wang H, et al. (2006) Fatty acid amide hydrolase deficiency limits early pregnancy events. *J Clin Invest* 116:2122–2131.
38. Meistrich ML (1977) Separation of spermatogenic cells and nuclei from rodent testes. *Methods Cell Biol* 15:15–54.
39. Stabile M, et al. (2008) Fertility in a i(Xq) Klinefelter patient: Importance of XIST expression level determined by qRT-PCR in ruling out Klinefelter cryptic mosaicism as cause of oligozoospermia. *Mol Hum Reprod* 14:635–640.
40. Pfaffl MW, Horgan GW, Dempfle L (2002) Relative expression software tool (REST) for group-wise comparison and statistical analysis of relative expression results in real-time PCR. *Nucleic Acids Res* 30:e36.